PHYSICAL REVIEW E **78**, 015301(R) (2008)

Slip coefficient in nanoscale pore flow

Vlad P. Sokhan*
National Physical Laboratory, Hampton Road, Teddington TW11 0LW, United Kingdom

Nicholas Quirke†
Department of Chemistry, Imperial College London, London SW7 2AY, United Kingdom

(Received 12 May 2008; published 2 July 2008)

The hydrodynamic solutions based on Maxwell's boundary conditions include an empirical slip coefficient (SC), which depends on properties of the adsorbate and adsorbent. Existing kinetic theory derivations of the SC are usually formulated for half-space flow and do not include finite-size effects, which dominate the flow in nanopores. We present an expression for the SC applicable to flow in nanoscale pores, which has been verified by nonequilibrium molecular-dynamics simulation. Our results show that the slip coefficient depends strongly on the pore width for small pores tending to a constant value for pores of width >20 molecular diameters for our systems, in contrast to the linear scaling predicted by Maxwell's theory of slip.

DOI: 10.1103/PhysRevE.78.015301 PACS number(s): 47.15.gm, 05.20.Jj, 47.11.Mn, 66.20.−d

Many recent experiments on nanoscale fluid flow of Newtonian liquids [1,2] and related simulation studies [3–6] support Maxwell's prediction of the possibility of molecular slip at a gas-solid interface [7]. It is known to exist where the Knudsen number, defined as the dimensionless ratio of molecular free path to some characteristic length, $\mathrm{Kn}=\lambda/L$, is non-negligible, and is usually associated with low densities where λ is large. However, in narrow capillaries (where L is small), slip can be observed even at liquid densities. In the general case, it is characterized by a slip coefficient, l_s [7,8], which in the absence of temperature gradients relates the collective molecular velocity at the wall, the slip velocity, to the shear rate, $\mathbf{u}_s = l_s \nabla \mathbf{u}$ [7]. Using kinetic theory, Maxwell derived a microscopic expression for the slip coefficient [7], which can be written as

$$l_s = \lambda\left(\frac{2}{\alpha} - 1\right), \tag{1}$$

where $\lambda = 2\eta/\rho\bar{c}$ is the mean free path, η is the shear viscosity, ρ is mass density of the fluid, and $\bar{c}$ is the mean speed of the molecules. Considering only two types of wall collision, specular and diffuse (Knudsen) reflection, he introduced a coefficient α that defines a fraction of specularly reflected molecules. In a more broad sense, α defines the fraction of the flux of tangential momentum transmitted in collisions and is often called the "accommodation coefficient" (TMAC) [8]. Its value is defined by the details of the solid-fluid interactions, and Eq. (1) implies finite slip even for purely diffusive reflections ($\alpha=1$). For a specularly reflecting surface, the slip coefficient diverges since the fluid cannot grip the surface.

Slip in nanoscale fluid flow depends on many parameters including surface roughness [6], electric properties of the interface [9], wetting conditions [5], and chemical patterning of the surface [10], and is a nonlinear function of the dynamic state [11]. Application of the generalized Navier-Stokes (NS) hydrodynamics to problems of fluid flow on the nanoscale is an attractive but highly nontrivial task even in simple cases such as plane Poiseuille flow. An accurate solution requires knowledge of the material parameters of the fluid as a function of local density, which deviates from its bulk value in the proximity of the interface. As a result, the velocity profile in narrow pores also deviates from the macroscopic prediction [12]. The usual approach is to regard the fluid as incompressible and to replace the complex nonuniform flow problem plus simple no-slip boundary conditions with a simple flow problem but with boundary conditions, which has been called "exceedingly difficult" for theoretical investigation [8]. The discontinuity in the flow field is introduced in this approach in the same way the surface excess was introduced by Gibbs in his treatment of interface boundaries at equilibrium as illustrated in Fig. 1 for the case of plane Poiseuille flow in the z direction ($\mathbf{u}=\{0,0,u_z\}$) between walls at $y=\pm h$, where the symmetry of the solution was taken into account and only one-half was plotted. We emphasize that the finite slip u_s that appears in this approach is a purely artificial device introduced only to match the approximate solution with the solution of the full problem in

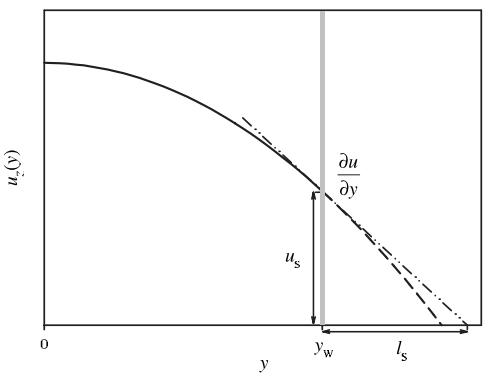

FIG. 1. Full line, velocity profile for the plane Poiseuille flow with surface slip; dashed line, extrapolated velocity profile. Vertical gray line marks the position of the solid. Dash-dotted line denotes the velocity gradient at the wall. Also shown are slip velocity, u_s, and slip coefficient, l_s.

*vlad.sokhan@npl.co.uk
†Also at Department of Physics, University College, Dublin, Ireland.

the middle part of the channel. The full solution for the continuum velocity field does decay to zero at the wall, as required by continuity of stresses in classical hydrodynamics [13]. Note, however, that although the velocity field is defined everywhere where the fluid density is nonzero, it cannot be measured in experiment or statistical particle-based simulation with a continuous solid-fluid potential in the regions where the particle Boltzmann factor is diminishingly small but still nonzero. The limiting value of the velocity field is therefore not observable due to finite sampling of the statistical ensemble.

There have been a number of attempts to estimate the TMAC from kinetic theory [14,15] and using molecular-dynamics (MD) simulation of simple liquids [5,16,17]. However, the results obtained by different groups and using different methods are inconclusive [1], with large scatter in reported values of slip coefficient spanning two orders of magnitude. The agreement between recent experiments with various surfaces [18–21] and theory is also poor, with experimental values for α generally higher than the corresponding theoretical expectations [15,16,18]. One of the limitations of the original Maxwell model is that it was developed to solve the half-space flow, or Kramers, problem [8] in the dilute gas regime and assuming that the TMAC is a local property. The collision flux that transmits the stress to the wall is independent of the pore width, and therefore the momentum transferred in each collision increases with the pore width and hence is a nonlocal property for the systems studied here.

In this paper, we present a method of calculating the slip coefficient that does not require assumptions about the type of wall collisions, thus avoiding the necessity of calculating the TMAC. We illustrate it on a simple case of gravity-driven plane Poiseuille flow in a pore of width $H=2h$ and with acceleration due to an external field $\mathbf{g}=\{0,0,g\}$ as sketched in Fig. 1. The method is equally applicable to structured and patterned surfaces and can be extended to a more general case of Poiseuille flow induced by a pressure gradient using the equivalence between the pressure gradient and gravity-driven force in the direction of flow [13].

It is often convenient to reformulate the slip velocity problem (Dirichlet boundary condition) in terms of interfacial viscosity (Neumann boundary condition) and the lateral wall stress. This idea goes back to Navier [22], who obtained the boundary condition for the velocity field on the basis of particle arguments (cf. the last equation on p. 415 in [22]) as

$$\eta \left.\frac{\partial u_z(y)}{\partial y}\right|_{y_w} = \beta u_z(y_w), \tag{2}$$

where his parameter β is related to the interfacial shear viscosity η via $l_s=\eta/\beta$. Note that for nonlinear velocity profiles, as for Poiseuille flow, the slip coefficient, l_s (shown in the figure), is different from the slip length, defined as the distance from the wall where the extrapolated velocity profile vanishes. However, if the difference between them is small, simple geometric consideration allows us to establish the relationship between the two types of boundary condition.

Neglecting viscous dissipation, the wall shear stress in terms of the external driving force acting on fluid particles, which in this case is simply $\sigma_{yz}=\rho g h$ [23], can be equated with the Stokesian drag force per unit area exerted on the wall by the moving fluid [24],

$$\sigma_{yz} = -\frac{F_S}{2A} = \frac{Mu}{2A\tau} \equiv \frac{\rho u h}{\tau}, \tag{3}$$

where A is the area of one wall, M is the total mass of the fluid in the pore, $u \equiv h^{-1}\int_0^h u_z(y)dy$ is the mean fluid velocity, and the relaxation time τ can be calculated in equilibrium molecular dynamics (EMD) simulation from the Langevin equation for the fluid subsystem considered as a single Brownian particle using the fluctuation-dissipation theorem. It was shown recently [25] that the fluid velocity autocorrelation function decays exponentially,

$$C(t) = M^{-1}kT\exp(-t/\tau), \tag{4}$$

and this provides a simple way to determine τ in an equilibrium simulation by fitting a one-parameter exponential to velocity autocorrelation data. From the above two expressions for the wall stress, a simple relationship between the acceleration due to the external force and the fluid velocity,

$$u = \tau g, \tag{5}$$

can be established. This surprisingly simple result shows that within the limits of the linear regime [11], the rate of fluid flow in nonequilibrium steady state can be estimated from the characteristic time of the decay of fluctuations at equilibrium.

The slip velocity can be obtained from the hydrodynamic solution,

$$u_z(y) = \frac{\rho g}{2\eta}(h^2 - y^2) + u_s, \tag{6}$$

by using Eq. (5) and the definition of u,

$$u_s = \left(\tau - \frac{\rho h^2}{3\eta}\right)g, \tag{7}$$

and by substituting it into the definition of the slip coefficient, $l_s=-(\partial u/\partial y|_h)^{-1}u_s$, one obtains finally for the slip length

$$l_s = \frac{\tau\eta}{\rho h} - \frac{h}{3}. \tag{8}$$

This is the main result. It shows that the slip coefficient is independent of the external force (flux), but depends nonlinearly on the pore width, both directly and, as will become clear later, indirectly through the relaxation time τ. In order to establish a connection with Maxwell's result, the relaxation time can be expressed [25] in terms of wall collision frequency per particle, f_0, and the TMAC, $\tau=(f_0\alpha)^{-1}$. Taking the kinetic theory expressions for the wall collision, $f_0=\bar{c}/4h$, and the Chapman-Cowling expression for the viscosity [8], $\eta=\rho\bar{c}\lambda/2$, one obtains the expression for the slip coefficient,

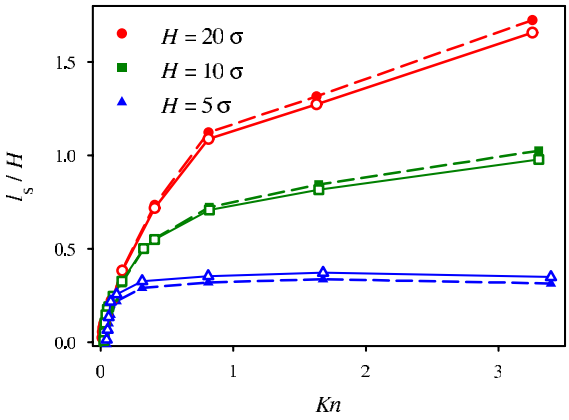

FIG. 2. (Color online) Slip coefficients calculated directly in NEMD (filled symbols and dashed lines) and estimated from the relaxation time [Eq. (8)] (open symbols and full lines) as a function of Knudsen number for three pore widths. Lines are drawn to guide the eye.

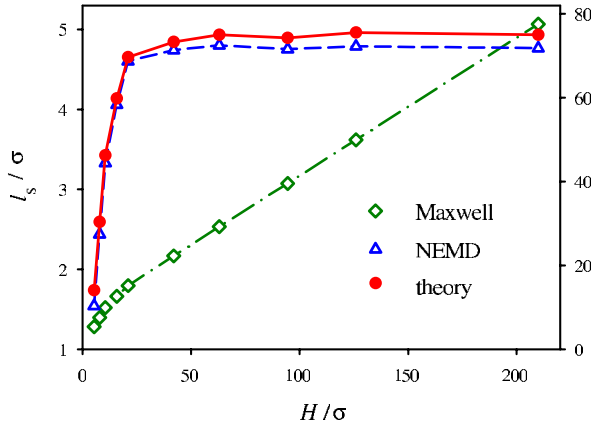

FIG. 3. (Color online) Slip coefficients (left scale) calculated directly in NEMD (triangles) and estimated from the relaxation time [Eq. (8)] (circles) as a function of pore width. For comparison, slip coefficients estimated from Maxwell's theory, Eq. (1) (diamonds) are also shown (right scale). Lines are drawn to guide the eye.

$$l_s = \lambda \frac{2}{\alpha} - \frac{h}{3}, \tag{9}$$

which can now be compared with Maxwell's result (1). The differences between the two results are elucidated below in the discussion of the results of molecular simulation. We emphasize here that we used the kinetic theory expression for f_0 and η in deriving Eq. (9) only to make the same level of approximation as was used in deriving Eq. (1).

In order to study the Knudsen number dependence of the slip coefficient, two series of EMD runs were performed in which the relaxation time was calculated. In the first series, the Kn was varied by changing the mean density of the system (the mean free path) in a pore of fixed width. In the second, performed at constant normal pressure, the pore width (the characteristic length) was varied. The slip coefficient estimated using Eq. (8) was compared with the values obtained directly in the parallel set of nonequilibrium molecular dynamics (NEMD) simulations of the Poiseuille flow for the same systems.

The system consists of supercritical Lennard-Jones (LJ) fluid, confined between two walls modeled by a rigid triangular lattice of atoms situated at $y_w = \pm h$, and periodically replicated along x and z axes to avoid edge effects. All interactions in the system were of the LJ form, $U(r) = 4\varepsilon[(\sigma/r)^{12} - (\sigma/r)^6]$, where ε and σ are the usual energy and length parameters. Their values for the fluid-fluid interactions define the corresponding scales, and in the following reduced units [26] are used, denoted by the asterisk. The solid-fluid interaction parameters in these units were taken as $\varepsilon_{sf} = 0.4348\varepsilon$ and $\sigma_{sf} = 0.9462\sigma$, and the surface number density of the solid was $n_s\sigma^2 = 1.105$ as in our earlier study [25], where more details about the system and the numerical scheme can be found. All MD calculations were performed using the classical molecular dynamics software package MDL [27]. The nonequilibrium steady-state conditions were realized by placing the fluid in a uniform external field parallel to the walls and coupling all fluid degrees of freedom to a Nosé-Hoover thermostat at $T = 2.026\varepsilon k^{-1}$, where k is the Boltzmann constant. The simulation cell was of dimensions $20.181\sigma \times H \times L_z$, where the dimension in the flow direction, L_z, was scaled with the density to keep the number of particles in the system around 2500. The time step was $\Delta t^* = 7.28 \times 10^{-3}$ in LJ units and the integration time in each case was not less than 3.64×10^5 (50 M steps). The value of the acceleration due to the external force was varied between $g^* = 4 \times 10^{-3}$ and 0.04 in order to keep the fluid velocity below $u^* = 0.2$. The steady states reported here are known to be well within the Newtonian regime [28] and the slip velocity in the linear regime [11]. To simplify the comparison, all flow-related properties were scaled to a common value $g^* = 4.95 \times 10^{-3}$.

In the first series, three pore widths were considered, $H = 5.328\sigma$, 10.499σ, and 20.997σ (in the future denoted as 5σ, 10σ, and 20σ for brevity), and several number densities ranging from $n^* = 0.02$ ($n^* = m^{-1}\rho\sigma^3$), corresponding to the rarefied fluid at Kn = 3.4 for a narrow pore (where we used the kinetic theory expression for the mean free path and the hard-sphere diameter for LJ [29]) to a dense state of $n^* = 0.8$, which for a wide pore gives Kn = 0.013, thus spanning more than two orders of magnitude of Knudsen numbers. In all cases, the Reynolds number defined as the ratio of inertial and viscous forces, $\mathrm{Re} = \rho u H/\eta$, was kept small, $\mathrm{Re} < 10$.

The shear viscosity of the fluid that enters Eq. (8) can be accurately estimated in EMD simulation from the stress autocorrelation function using Green-Kubo relations, as has been recently shown for the bulk LJ fluid [30]. In NEMD simulation, it can also be calculated from the NS hydrodynamics using the quadratic fit to NEMD velocity profiles. To simplify the calculations, we used an empirical equation of state for the bulk fluid viscosity [31] at a density equal to the mean density in the central part of the channel, where it is uniform, to fit the simulated data at the required temperature. The agreement with NEMD values for the two wider pores is excellent, with differences typically smaller that statistical uncertainty, ~1%, for $n^* > 0.2$. Deviation of the order of 10% from the bulk values for the $H = 5\sigma$ pore is due to the overlap of adsorbed layers at two surfaces and to inaccuracy

in determination of the reference bulk density. At lower densities, when $\mathrm{Kn} \geq 1$, the viscosity in the pore deviates markedly from bulk values.

The ratio of the slip coefficients to the pore width, calculated in NEMD and estimated from the relaxation times and bulk viscosities at densities equal to that in the middle of the pore using Eq. (8), is compared in Fig. 2 for three pore widths. The relaxation time was estimated from the exponential fit to the collective velocity autocorrelation function calculated in EMD simulation using the procedure described elsewhere [25]. The statistical uncertainty in all cases is of the order of symbol size and is slightly higher for wider pores since the longer relaxation times in this case require more accurate estimation of the velocity autocorrelation time at long correlation times. For all pores, the slip coefficients calculated using the two routes agree within statistical uncertainties.

At low fluid densities (large Kn), the TMAC changes insignificantly with Kn [25], and both Eqs. (1) and (9) predict linear dependence of the slip coefficient on the Knudsen number in this region. For two wider pores, this behavior is indeed observed for $\mathrm{Kn} > 1$. For the narrowest pore, the increase in Kn is balanced by the increase in TMAC at low densities rendering the slip length effectively independent of Kn.

The results also show that for the systems with the same Knudsen number, the slip coefficient increases with the pore width. To study the pore width dependence of the slip coefficient in more detail, a second series of calculations was performed at the constant normal pressure that corresponds to reduced density of $n^*=0.125$ up to the pore width $H=210\sigma$. The difference from Maxwell's results using Eq. (1) is clearly seen in Fig. 3. The results estimated using Eq. (8) agree with those obtained directly in NEMD within statistical uncertainty and show that after initial increase, the slip coefficient reaches its limiting value at about $H=25\sigma$, which for the density chosen is $l_s=4.77(2)\sigma$. In contrast, Maxwell's theory predicts a linear scaling of the slip coefficient with pore width due to a decrease in α, and for the widest pore studied Eq. (1) gives the value $l_s=77.5\sigma$, which is more than an order of magnitude higher than the NEMD result (note the difference in scales). It is expected to level out at a much larger hydrodynamic scale due to dissipative processes in the fluid.

In summary, we provide a way to calculate the slip coefficient that requires only two material parameters: shear viscosity, which can be taken from the bulk equation of state for the viscosity, and relaxation time, which is a function of the thermodynamic state of the liquid and also depends on the pore dimensions. Crucially, it does not depend on the dynamic state and can be calculated from the collective velocity autocorrelation function in equilibrium simulation. Our results show that the slip coefficient increases almost linearly with the pore width before reaching a plateau at $\sim 20\sigma$, indicating that there is a characteristic length associated with this change.

This work was funded as part of the National Physical Laboratory's Strategic Research Programme and EPSRC under Grant No. GR/N64809/01.

[1] E. Lauga, M. P. Brenner, and H. A. Stone, in *Handbook of Experimental Fluid Dynamics*, edited by C. Tropea, A. Yarin, and J. F. Foss (Springer, New York, 2007), Chap. 19.
[2] C. Neto, D. R. Evans, E. Bonaccurso, H.-J. Butt, and V. S. J. Craig, Rep. Prog. Phys. **68**, 2859 (2005).
[3] J.-L. Barrat and L. Bocquet, Faraday Discuss. **112**, 119 (1999).
[4] Y. Zhu and S. Granick, Phys. Rev. Lett. **87**, 096105 (2001).
[5] V. P. Sokhan, D. Nicholson, and N. Quirke, J. Chem. Phys. **115**, 3878 (2001).
[6] C. Cottin-Bizonne, J.-L. Barrat, L. Bocquet, and E. Charlaix, Nat. Mater. **2**, 237 (2003).
[7] J. C. Maxwell, Philos. Trans. R. Soc. London **170**, 231 (1879).
[8] C. Cercignani, *Mathematical Methods in Kinetic Theory* (Plenum, New York, 1969).
[9] L. Joly, C. Ybert, E. Trizac, and L. Bocquet, J. Chem. Phys. **125**, 204716 (2006).
[10] T. Qian, X.-P. Wang, and P. Sheng, Phys. Rev. E **72**, 022501 (2005).
[11] P. A. Thompson and S. M. Troian, Nature **389**, 360 (1997).
[12] K. P. Travis and K. E. Gubbins, J. Chem. Phys. **112**, 1984 (2000).
[13] G. K. Batchelor, *An Introduction to Fluid Dynamics* (Cambridge University Press, Cambridge, 1970).
[14] D. Nicholson and S. K. Bhatia, J. Membr. Sci. **275**, 244 (2006).
[15] H. Ambaye and J. R. Manson, Phys. Rev. E **73**, 031202 (2006).
[16] V. P. Sokhan, D. Nicholson, and N. Quirke, J. Chem. Phys. **117**, 8531 (2002).
[17] G. Arya, H. C. Chang, and E. J. Maginn, Mol. Simul. **29**, 697 (2003).
[18] H. Legge, J. R. Manson, and J. P. Toennies, J. Chem. Phys. **110**, 8767 (1999).
[19] E. B. Arkilic, K. S. Breuer, and M. A. Schmidt, J. Fluid Mech. **437**, 29 (2001).
[20] O. V. Sazhin, S. F. Borisov, and F. Sharipov, J. Vac. Sci. Technol. A **19**, 2499 (2001).
[21] B.-Y. Cao, M. Chen, and Z.-Y. Guo, Appl. Phys. Lett. **86**, 091905 (2005).
[22] C. L. M. H. Navier, Mem. Acad. Sci. Inst. Fr. **6**, 389 (1827).
[23] V. P. Sokhan, N. Quirke, and J. Greenwood, Mol. Simul. **31**, 535 (2005).
[24] V. P. Sokhan, D. Nicholson, and N. Quirke, J. Chem. Phys. **120**, 3855 (2004).
[25] V. P. Sokhan and N. Quirke, Mol. Simul. **30**, 217 (2004).
[26] M. P. Allen and D. J. Tildesley, *Computer Simulation of Liquids* (Clarendon, Oxford, 1987).
[27] Molecular Dynamics Laboratory (MDL) is a classical molecular-dynamics package for molecular systems developed by V. Sokhan at NPL within the Strategic Research Fellowship Programme.
[28] J.-L. Barrat and L. Bocquet, Phys. Rev. Lett. **82**, 4671 (1999).
[29] D. Heyes, J. Chem. Soc., Faraday Trans. 2 **84**, 705 (1988).
[30] K. Meier, A. Laesecke, and S. Kabelac, J. Chem. Phys. **121**, 3671 (2004).
[31] L. V. Woodcock, AIChE J. **52**, 438 (2005).